Published in final edited form as:
Circulation. 2014 March 11; 129(10): 1092–1103. doi:10.1161/CIRCULATIONAHA.113.003077.

Missense Mutations in Plakophilin-2 Cause Sodium Current Deficit and Associate with a Brugada Syndrome Phenotype

Marina Cerrone, MD[1,2,*], **Xianming Lin, PhD**[1,*], **Mingliang Zhang, PhD**[1], **Esperanza Agullo-Pascual, PhD**[1], **Anna Pfenniger, MD,PhD**[1], **Halina Chkourko Gusky, PhD**[1], **Valeria Novelli, PhD**[3], **Changsung Kim, PhD**[4,5], **Tiara Tirasawasdichai, BA**[4], **Daniel P Judge, MD**[6], **Eli Rothenberg, PhD**[7], **Huei-Sheng Vincent Chen, MD,PhD**[4], **Carlo Napolitano, MD,PhD**[3], **Silvia Priori, MD,PhD**[1,2,3], and **Mario Delmar, MD,PhD**[1]

[1]Leon H Charney Division of Cardiology, NYU School of Medicine, New York, NY

[2]Cardiovascular Genetics Program, NYU School of Medicine, New York, NY

[3]Molecular Cardiology, Maugeri Foundation; Pavia, Italy

[4]Del E. Webb Center for Neuroscience, Aging & Stem Cell Research, Sanford-Burnham Medical Research Institute, La Jolla, CA

[5]Department of Bioscience and Biotechnology, Sejong University, Seoul, Korea

[6]Division of Cardiology, Johns Hopkins University School of Medicine, Baltimore, MD

[7]Department of Pharmacology, NYU School of Medicine, New York, NY

Abstract

Background—Brugada syndrome (BrS) primarily associates with loss of sodium channel function. Previous studies showed features consistent with sodium current (I_{Na}) deficit in patients carrying desmosomal mutations, diagnosed with arrhythmogenic cardiomyopathy (AC; or arrhythmogenic right ventricular cardiomyopathy, ARVC). Experimental models showed correlation between loss of expression of desmosomal protein plakophilin-2 (PKP2), and reduced I_{Na}. We hypothesized that *PKP2* variants that reduce I_{Na} could yield a BrS phenotype, even without overt structural features.

Methods and Results—We searched for *PKP2* variants in genomic DNA of 200 patients with BrS diagnosis, no signs of AC, and no mutations in BrS-related genes *SCN5A, CACNa1c, GPD1L and MOG1*. We identified 5 cases of single amino acid substitutions. Mutations were tested in HL-1-derived cells endogenously expressing $Na_V1.5$ but made deficient in PKP2 (PKP2-KD). Loss of PKP2 caused decreased I_{Na} and $Na_V1.5$ at site of cell contact. These deficits were restored by transfection of wild-type PKP2 (PKP2-WT), but not of BrS-related PKP2 mutants. Human induced pluripotent stem cell cardiomyocytes (hIPSC-CMs) from a patient with PKP2 deficit showed drastically reduced I_{Na}. The deficit was restored by transfection of WT, but not BrS-related PKP2. Super-resolution microscopy in murine PKP2-deficient cardiomyocytes related I_{Na} deficiency to reduced number of channels at the intercalated disc, and increased separation of microtubules from the cell-end.

Correspondence: Mario Delmar MD,PhD, The Leon H Charney Division of Cardiology, New York University School of Medicine, 522 First Avenue. Smilow 805, New York NY 10016, Phone: 212-263-9492, Fax: 212-263-3972, mario.delmar@nyumc.org.
*contributed equally

Conflict of Interest Disclosures: None.

Conclusions—This is the first systematic retrospective analysis of a patient group to define the co-existence of sodium channelopathy and genetic PKP2 variations. *PKP2* mutations may be a molecular substrate leading to the diagnosis of BrS.

Keywords

plakophilin-2; arrhythmogenic right ventricular dysplasia/cardiomyopathy; Brugada syndrome; sodium channels; desmosomes arrhythmia

INTRODUCTION

Mutations in the *PKP2* gene, coding for the desmosomal protein plakophilin-2 (PKP2), cause the most prevalent genetic form of Arrhythmogenic Cardiomyopathy (AC, also known as “arrhythmogenic right ventricular cardiomyopathy”, ARVC)[1]. Recent studies have demonstrated that PKP2 not only participates in intercellular coupling[2, 3], but it also interacts, directly or indirectly, with the voltage-gated sodium channel (VGSC) complex[4, 5]. We have shown that siRNA-mediated loss of PKP2 expression in isolated cells affects the amplitude and kinetics of the sodium current (I_{Na}), and provided evidence that a mouse model haploinsufficient for PKP2 shows I_{Na} deficit, leading to flecainide-induced ventricular arrhythmias and sudden death[6]. Moreover, a recent analysis of human heart samples found that the abundance of the immunoreactive signal for the cardiac alpha subunit of the sodium channel, $Na_V1.5$, was decreased in 65% of AC patients tested[7]. Overall, the data support the notion that loss and/or impairment of $Na_V1.5$ function at the intercalated disc might be a component of the molecular profile of AC associated with mutations in PKP2. Yet, loss of function of the sodium channel has been primarily associated with the phenotype of a different inherited arrhythmia, namely Brugada syndrome (BrS)[8]. Here, we speculate that variants of PKP2 that decrease I_{Na} amplitude could yield a BrS phenotype, even in the absence of cardiomyopathic features characterizing AC.

We sought to identify *PKP2* variants in genomic DNA of patients with clinical diagnosis of BrS and without mutations in BrS-related genes *SCN5A*, *CACNa1c*, *GPD1L and MOG1*. We screened the open reading frame of *PKP2* samples from 200 patients with diagnosis of BrS and without clinical signs of AC and identified in 5/200 (2.5%) the presence of a single nucleotide replacement leading to an amino acid substitution. We speculated that those variants could be sufficient to affect VGSC function. To characterize the electrophysiological and molecular consequences of these mutants we developed a new HL-1-derived cardiac cell line that endogenously expresses $Na_V1.5$ but is deficient in PKP2 (PKP2-KD). As previously reported in both neonate and adult cardiac myocytes[4–6], loss of PKP2 in these cells caused a decrease in the magnitude of I_{Na} and decreased abundance of $Na_V1.5$ at the site of cell contact. Transient transfection of wild-type (WT) PKP2 restored VGSC function and $Na_V1.5$ membrane localization; yet, transfection of PKP2 mutants found in patients with BrS failed to restore function and localization of $Na_V1.5$, even if co-expressed with the WT construct. Similarly, human induced pluripotent stem cell cardiomyocytes (hIPSC-CMs) from a patient with PKP2 deficit showed drastically reduced I_{Na}. The deficit was restored by transfection of WT, but not BrS-related PKP2. Further mechanistic insight was gained from the study of PKP2 heterozygous-null (PKP2-Hz) ventricular myocytes. Using super-resolution microscopy and scanning patch clamp methods[3, 9] we observed that I_{Na} deficiency was specific to the intercalated disc (ID) and resulted from reduced number of functional channels. We also observed increased separation between the microtubule plus-end, and N-cadherin containing plaques. Overall, our data show for the first time that a clinical phenotype consistent with diagnosis of BrS can associate in 2–3% of patients with missense variants in a desmosomal gene that, in turn,

causes I_{Na} deficit in an experimental system. The possible implications of this finding to our understanding of BrS and AC as separate clinical entities are discussed.

METHODS

Detailed methods are provided in online supplement (OS).

Study population and genetic screening

A total of 200 de-identified patients [179 males] from the Registry of the Molecular Cardiology Laboratories, Maugeri Foundation, Pavia, Italy were included in this study. Patients were selected based on clinical definite diagnosis of BrS and absence of mutations on SCN5A, CACNa1c. Genes GPD1L and MOG1 were subsequently screened and no mutation was found. DNA extraction, amplification and direct sequencing of the entire open reading frame/splice junction of PKP2 followed standard techniques.

Experiments in HL-1 cells

Cell culture and generation of PKP2-deficient HL1 cells—HL-1 is a cell line derived from the AT-1 mouse atrial cardiomyocyte tumor lineage[10]. Cell culture conditions followed those previously described[10]. To generate stable PKP2-deficient cells (PKP2-KD), a lenti-PKP2-shRNA clone (ID TRCN0000123349) was packaged using a TransLenti Viral Packaging System (Open Biosystem). A separate line expressing a non-silencing Lenti vector (PKP2-φKD) was used as a control.

Transient transfection of PKP2 constructs—PKP2-KD cells were transiently transfected with a vector containing cDNA for human PKP2 concatenated to the N-terminal of mCherry, for identification of transfected cells. The following PKP2 variants were generated: D26N, Q62K, S183N, M365V, T526A and R635Q. A plasmid coding only for mCherry was used as control. Plasmids were introduced using the Lipofectamine 2000 reagent (Life Technologies).

Immunochemical analysis of HL1 cells—Samples were imaged using a Leica SP5 confocal microscope. Co-localization was quantified by Pearson's co-localization coefficient, as described[11], using the Intensity Correlation Analysis Plugin in the WCIF Image J software (NIH).

Real Time PCR—Total RNA was extracted using RNeasy Mini Kit (QIAGEN). The relative quantitation (RQ) of comparative cycle threshold (CT) was utilized for analysis.

Whole-cell patch-clamp—Whole-cell I_{Na} recordings were conducted using an Axon multiclamp 700B Amplifier and a pClamp system (versions 10.2, Axon Instruments, Foster City, CA); recording solutions and protocols in online supplement.

hIPSC-CMs

AC-hIPSC-CMs were obtained from line JK#11, derived from a patient with clinical diagnosis of AC and a homozygous c.2484C>T mutation in *PKP2* causing a cryptic splicing with a 7-nucleotide deletion in exon 12. Extensive characterization of the cellular/molecular phenotype in[12, 13]. Details in online supplement. We performed *PKP2* rescue experiments with lentiviral constructs containing WT-*PKP2* or *PKP2* with a c.1904 G>A mutation (p.R635Q), tagged with green fluorescent proteins (GFP) for verification, according to methods described previously[12].

Experiments in PKP2 heterozygous-null (PKP2-Hz) mice

The PKP2-Hz murine model has been described before[6]. All procedures conformed to the Guide for the Care and Use of Laboratory Animals published by the US National Institutes of Health (NIH Publication 58-23, revised 1996). Dissociation of single adult ventricular myocytes, recording by macropatch and immunolocalization of relevant proteins followed standard procedures outlined in online supplement.

Super-resolution scanning patch clamp—This method combines scanning ion conductance microscopy (SICM) with cell-attached patch clamp technology for recording of ion channels at a particular subcellular location. Detailed methods in[9]. A brief description in online supplement.

Super-resolution fluorescence microscopy: direct Stochastic Optical Reconstruction Microscopy (dSTORM)—To co-localize clusters of microtubule-plus end binding protein (EB-1) and N-cadherin in single isolated ventricular myocytes we used two-color dSTORM. Our spatial resolution in the X-Y plane was estimated at ~20 nm. Detailed methods in[3]. Brief description in online supplement.

Statistical analysis

Each individual comparison was limited to two data sets (e.g., wild-type versus mutant). Results were statistically analyzed without assuming a defined structure in the data set (non-parametric statistics). Significance was calculated by a Mann-Whitney-Wilcoxon (MWW) test to assess the null hypothesis that two populations were the same, against the alternative hypothesis that a particular population tended to have larger values than the other. No adjustments were made for multiple comparisons due to the nature of the study. Significance was defined by $p<0.05$. For all data plots involving statistics, a dot plot format was used: open circles represent individual data points, the black circle is the median value, and lower and upper horizontal lines indicate first and third quartiles, respectively.

RESULTS

Genetic Screening

We found five single amino acid substitutions on PKP2 in five unrelated individuals. Variant Q62K (c.185 C>A, on exon 1), was reported in patients with diagnosis of AC, and in 3/12602 (MAF 0.02%)[14] alleles screened in the NHLBI Exome Sequencing Project database (EVS, http://evs.gs.washington.edu/EVS/). It is defined as variant of unknown significance (VUS), because of contrasting data on potential deleterious effect[15]: absence of co-segregation with clinical phenotype in some cohorts[16], concomitant presence of additional desmosomal mutations in some affected individuals[17], and detection in individuals without overt clinical phenotype.[18] Four other variants were novel. Three, S183N (c.548G>A); T526A (c.1576A>G) and R635Q (c.1904G>A) are unreported variants, absent in 200 healthy controls screened in our laboratory and 6500 healthy controls reported in EVS. The fifth variant, M365V (c. 1093A>G) is novel, not present in our controls and reported in 2/13004 alleles of the EVS (MAF 0.01%)[14]. Amino acid substitution D26N [rs143004808] was found in 7 unrelated patients. This variant is present in healthy individuals and not thought to cause disease[15]. It was therefore used as additional control in the cell expression systems.

Clinical characteristics

All patients were evaluated at the Molecular Cardiology Program, Fondazione Maugeri, Pavia, Italy. They were diagnosed with BrS based on clinical history, diagnostic ECG

pattern either spontaneous or after flecainide challenge and absence of structural cardiomyopathy at echocardiogram or cardiac magnetic resonance imaging. Detailed clinical data are presented in Supplemental Table 1. Briefly, 3 patients had a saddle-back ECG in baseline with conversion into coved-type diagnostic ECG pattern after flecainide infusion,[19] while two showed an abnormal coved-type pattern at the surface ECG (Figure 1 ad Supplemental Figure 1). Three had history of syncope at rest or after large meal, a feature characteristic of the disease[19]. In one (mutation carrier S183N), the ECG pattern was elicited by a febrile episode and associated with frequent PVCs[19]. One patient (mutation T526A) received an ICD after experiencing 2 syncopal episodes at rest; two months later, he experienced cardiac arrest at rest, with evidence of ventricular fibrillation, treated by the ICD. The carrier of mutation R635Q had 2 syncopal episodes at rest and spontaneous coved-type diagnostic ECG, and received a prophylactic ICD. His family members agreed to undergo cascade genetic screening. The asymptomatic mother did not carry the R635Q variant. His father, who had history of syncopal episodes at rest, and his brother, asymptomatic but with suspect ECG, resulted gene-carriers. The brother underwent flecainide challenge that resulted positive, confirming the genetic diagnosis. The paternal grandfather had history of syncope and died suddenly during sleep, but DNA was not available for testing. Altogether, these data show co-segregation between clinical phenotype and presence of variant R635Q, supporting the hypothesis of a deleterious, disease-causing effect.

The sodium channel complex, and PKP2 in HL-1 cells

Assessment of the relation between PKP2 primary sequence and I_{Na} required a system to test sequence variations in *PKP2* in the setting of stable, endogenous $Na_V1.5$ expression. As a line of cardiac origin[10], HL-1s present characteristics of differentiated myocytes, including expression of $Na_V1.5$[20]. As shown in Figure 2A (black symbols), voltage clamp steps elicited a voltage-dependent, fast inactivating inward current, as previously reported[20] (see also Supplemental Figure 2A,B). RT-PCR confirmed transcription of *SCN5A*. The abundance of *SCN5A* was three orders of magnitude higher than that of *SCN1A*, *SCN3A* and *SCN8A* (Supplemental Figure 2C). Immunolocalization and Western blot experiments showed expression of $Na_V1.5$ (Supplemental Figure 2D,E). Similarly, we detected expression of PKP2, with undetectable levels of PKP1 or PKP3 by western blot (Supplemental Figure 2E,F). Next, we established the relation between PKP2 expression, and I_{Na}.

Generation of PKP2-deficient HL-1s. Relation between PKP2 expression, and I_{Na}

HL-1s were infected with lentivirus coding for PKP2-shRNA, or for a non-silencing oligonucleotide. In both cases, the puromicin-resistant gene was used for selection. The corresponding cell lines were dubbed PKP2-KD, and PKP2-φKD. Western blots showed the expected loss of PKP2 in PKP2-KD but not in PKP2-φKD cells (Supplemental Figure 3A). Interestingly, loss of PKP2 expression led to significant loss of average peak I_{Na} density (Figure 2A), similar to that reported in neonatal and adult ventricular myocytes[5]. No PKP2-dependent changes in voltage-dependence of steady-state inactivation, or time course of recovery from inactivation were detected (see Supplemental Figure 3B,C). We observed no change in $Na_V1.5$ abundance (Supplemental Figure 3A), but decreased co-localization of $Na_V1.5$ with N-cadherin at site of cell contact in PKP2-deficient cells (Figure 2B).

To confirm the relation between PKP2 expression and I_{Na}, PKP2-KD cells were transiently transfected with wild-type *PKP2* (PKP2-KD+PKP2-WT). To identify transfected cells, PKP2 was concatenated in its C-end with mCherry. Controls were transiently transfected with mCherry alone (PKP2-KD+mCherry). As shown in 2C, peak I_{Na} density in PKP2-KD +PKP2-WT cells was significantly larger than in PKP2-KD or in PKP2-KD+mCherry cells

(see also Supplemental Figure 3D,E). Thus, exogenous expression of PKP2-WT rescued I_{Na} deficiency consequent to loss of expression of endogenous *PKP2*. Consistent with this observation, the extent of co-localization of $Na_V1.5$ and N-cadherin was rescued by transfection of the wild-type construct, but not by transfection of mCherry cDNA (2D).

BrS-related PKP2 variants and the sodium channel

The cellular system described above allowed us to determine whether mutations in *PKP2* would alter the relation between PKP2 expression, and I_{Na}. We generated six constructs, all as mCherry concatenants: PKP2-D26N, PKP2-Q62K, PKP2-S183N, PKP2-M365V and PKP2-T526A and PKP2-R635Q. I_{Na} in cells transfected with PKP2 variants was compared with that in PKP2-KD cells transfected with PKP2-WT or with mCherry. For each experiment, PKP2-KD cells were split from the same flask, and divided for treatment with PKP2-WT, mCherry or the particular PKP2 mutant. I_{Na} was measured from all three conditions on each test day, to ensure consistency. For each set, data were normalized to the average value of peak I_{Na} density of the PKP2-KD+PKP2-WT group. In contrast with results from PKP2-WT-transfected cells, mutants PKP2-Q62K, PKP2-S183N, PKP2-M365V, PKP2-T526A and PKP2-R635Q failed to rescue the I_{Na} deficit observed in PKP2-KD cells (3A); steady-state inactivation and recovery from inactivation were not affected either by loss of PKP2 or by expression of mutants (see Supplemental Figure 4,5). Yet, variant PKP2-D26N, not thought to be causative of disease[15], behaved as PKP2-WT (Figure 3A; bottom right; cumulative data in 3B). Interestingly, similar trend was observed for N-cadherin/$Na_V1.5$ co-localization. Transient transfection of PKP2-WT, or PKP2-D26N, enhanced co-localization to levels significantly higher than those for any of five mutant PKP2 constructs (Supplemental Figure 6). Pearson's coefficient values, in 3C. Western blot showing equivalent levels of PKP2 expression, in Supplemental Figure 7.

Our results show I_{Na} deficit when PKP2 mutations were expressed in PKP2-null background. BrS patients, on the other hand, were heterozygous for the PKP2 variant. Additional experiments evaluated I_{Na} properties in HL1s when both, WT and PKP2-variant constructs were co-expressed (transfection at 1:1 ratio). As shown in Fig.4 (and Supplemental Figures 8,9,10), I_{Na} in cells co-expressing PKP2-WT and a BrS-related PKP2 variant was less than that recorded in cells expressing only the wild-type protein, or WT plus variant PKP2-D26N.

AC-hIPSC-CMs showed reduced I_{Na}, rescued by PKP2-WT but not by a PKP2-BrS variant

Our data show that loss of expression, as well as mutations in PKP2 lead to decreased I_{Na}. Yet, HL-1s derive from a murine atrial myxoma and as such, their behavior may differ from that of human cardiomyocytes. Therefore, we performed an additional I_{Na} rescue experiment using a previously characterized hIPSC-CM line from an AC patient with a homozygous loss-of-function *PKP2* mutation[12]. As shown in Fig.5, I_{Na} was significantly less in cells from the AC patient (AC-hIPSC-CMs) than in cells from control (H9 human embryonic stem cell-derived cardiomyocytes). More importantly, lentiviral transfection of PKP2WT but not of PKP2-R635Q significantly increased I_{Na} density. This confirms that I_{Na} depends on expression/structural integrity of PKP2.

Analysis of sodium channel functional expression in PKP2-Hz cardiomyocytes

Our data so far were obtained in cells in culture, which differ from adult cardiomyocytes in terms of structural organization/function of junctional complexes. To explore the mechanisms of PKP2-dependent I_{Na} deficiency, we used adult ventricular myocytes from PKP2-Hz mice.

Based on our results, we speculated that PKP2 regulates cell surface expression of functional sodium channels at the ID. As an initial approach, we quantified the amplitude of local I_{Na} using the macropatch technique[21]. The terms "ID" and "M" refer to recordings from the region previously occupied by the ID, and from the cell midsection, respectively (diagram to left of 6A). Figure 6A shows no difference in average peak I_{Na} amplitude recorded from the midsection of cells obtained from PKP2-Hz mice (red) or their control littermates (black). However, the amplitude of I_{Na} measured at the ID (Fig.6B) was significantly reduced in PKP2-Hz when compared to control (additional data in Supplemental Figures 11 and 12). Overall, we show that PKP2 deficit causes selective reduction of I_{Na} at the ID.

To discard the possibility that reduced I_{Na} was consequent to decreased single-channel unitary conductance, we recorded sodium channels from a small, highly localized area at the cell end using super-resolution scanning patch clamp[9]. A topology map of the cell end is shown in 6C and the unitary measurements in 6D. The data show that reduced I_{Na} in PKP2-deficient cells is consequent not to decreased unitary conductance (in fact, a small increase was detected), but to reduced number of available $Na_V1.5$ channels, specifically at the ID.

The reduced number of available channels could be consequent to decreased open probability of membrane-inserted channels, or to reduced presence of sodium channel-forming proteins. Following on our results in HL1s (Supplemental Figure 6), we assessed the extent of $Na_V1.5$/N-cadherin co-localization at the ID[22]. As shown in Fig.7, $Na_V1.5$/N-cadherin co-localization decreased in PKP2-Hz cells when compared to control, though the amount of total $Na_V1.5$ in the cell lysate was unaffected by PKP2 deficit[6]. Altogether, we propose that decreased I_{Na} amplitude in PKP2-deficient cells is consequent to decreased cell surface expression of $Na_V1.5$ at the ID.

PKP2 deficit causes separation of the microtubule plus-end from N-cadherin plaques

The results were consistent with a role for PKP2 in forward trafficking of $Na_V1.5$ (among other not mutually exclusive possibilities). Previous studies indicated that sodium channels are delivered to the cell membrane via the microtubule network[23, 24], and that microtubules at the ID anchor at N-cadherin-rich sites[25]. We therefore explored whether microtubule arrival to the ID was impaired in PKP2-Hz myocytes. Specifically, we used two-color dSTORM to determine the distance between the plus-end of microtubules (marked by immunoreactive EB-1; see, e.g[25]) and the cell end (defined by the midline of N-cadherin clusters; see OS for methods). Fig.8 shows an image of EB-1 and N-Cadherin signals acquired by conventional TIRF (panel A, left) and dSTORM (A, right). The improved resolution of dSTORM (~20 nm, versus ~300 nm in TIRF; see bottom panels in A) allowed us to accurately measure separation distances (B). As shown in C, PKP2 deficiency led to increased average distance between the leading edge of EB-1 clusters, and the N-cadherin plaque midline. These results indicate that PKP2 deficiency, directly or indirectly, affects the ability of microtubules to reach the ID, likely impairing delivery of proteins relevant for sodium channel function.

DISCUSSION

Previous studies demonstrated reduced $Na_V1.5$ at the ID in samples from patients with desmosomal mutations.[7] Experimental models have shown correlation between loss of PKP2 expression, and reduced I_{Na}[4–6]. This manuscript represents the first retrospective analysis of a patient group to define the co-existence of clinical sodium channelopathy (BrS) and genetic variation in PKP2. This is also the first study demonstrating that not only loss of PKP2, but also single amino acid mutations, can interfere with I_{Na}. Our results support the notion that, in some cases, mutations in PKP2 can be part of the BrS molecular substrate.

Limitations

We focused on detection of variants in one desmosomal gene (*PKP2*). As such, we did not examine the possibility of other desmosomal mutations. We based this choice on a) the body of experimental evidence associating PKP2 with sodium current function[4–7], b) the high frequency of PKP2 mutations when compared to other desmosomal genes[1] and c) the need for an in vitro cell system to test structure-function relation between a specific desmosomal protein, and the sodium channel. Thus, while additional studies have shown that overexpression of a desmoglein-2 mutation also leads to I_{Na} dysfunction[26], we did not expand our study in that direction due to the likely failure to maintain and successfully transfect healthy HL-1 cells in the absence of desmosomal cadherins.

Our patients did not have mutations in either *SCN5A* or *CACNA1C*, the two genes most commonly associated with BrS and the subject of standard test for clinical diagnosis[27]. We also confirmed absence of mutations on two additional -though rare- BrS genes coding for sodium channel interacting proteins, MOG1 and GPD1L. While variants in other genes have been found in BrS patients, their occurrence is rare[27]. As in those cases, we do not know if the PKP2 mutations reported here occur in the context of additional genetic differences. Indeed, there is a large number of known proteins (and likely, a large number of unknown ones) that can affect, directly or indirectly, I_{Na}. Rather than extending our search to the entire genome of each patient, we focused on one gene while acknowledging that the PKP2 variants found represent part of the substrate and yet, perhaps not the only mechanism, when it comes to the clinical phenomena observed.

Exogenous systems are often used to study ion channel structure-function. In most cases, non-cardiac cells are used. Here we chose a cardiac cell line, so that components of the VGSC complex would follow their native transcription/translation process. A great advantage of this system is that, for the first time, we were able to experimentally assess the relation between single amino acid PKP2 mutations, and VGSC function and localization in a cardiac cell. The system also has limitations, one of which is that, in its most direct application, it does not model heterozygocity (Figure 3). To circumvent this problem, we carried out co-expression experiments (Figure 4). The similarity between results (Figure 3 versus 4) may suggest a possible dominant negative effect of the mutant. However, our experimental conditions are too artificial to make such a conclusion. What we do show is that even in the presence of WT-PKP2, an I_{Na} deficit was detected.

Our results in HL1 cells were confirmed and expanded using the hIPSC-CM system (5). Technical complexities forced us to limit the test to one mutant. We chose mutation R635Q given that co-segregation data were also available (see Figure 1C). Our data show that the relation between PKP2 expression/primary sequence and I_{Na} is also present in human cardiac cells.

Because of the more defined compartmentalization of ID molecules, we chose PKP2-Hz cells to assess mechanisms by which PKP2 deficiency leads to I_{Na} deficit. We recognize that the mechanisms described here may be influenced by expression of a mutant allele. Future experiments will involve generation and characterization of a PKP2-knockin mouse model expressing one of these mutations. Overall, our results show a tight convergence across experimental models demonstrating the importance of PKP2 in the proper function of the sodium channel complex.

PKP2 and BrS

BrS is an inherited channelopathy characterized by ST segment elevation of coved morphology in right precordial leads, increased risk of ventricular tachycardia and

ventricular fibrillation and absence of cardiac structural disease[19]. *SCN5A* mutations account for ~20–25% of genotype-positive subjects[27], and about 4% of patients carry mutations in the *CACNA1c* gene. Several other genes have been associated with sporadic cases of BrS, but each one accounts for <2% of patients; as such, current guidelines do not advise to screen for them routinely in the general BrS population[27]. Overall only 25–30% of patients with clinical diagnosis of BrS have a known genotype, implying that additional, still undiscovered genes may be linked to this disease.

When BrS was initially described, some investigators proposed that this condition shared features with AC, thus opening the possibility that they represent two poles of a common spectrum ultimately leading to increased risk of sudden death[28]. In fact, on one side, some BrS patients show minor RV structural abnormalities[29] while on the other side, desmosomal mutation carriers can experience ventricular fibrillation and sudden death without overt structural disease[30–33]. Our study supports the notion that one gene (e.g., PKP2) can be an underlying factor in both ends of this spectrum. There are other cases where the same gene is involved in more than one clinical phenotype (partly depending on whether the mutation leads to loss or gain of function): SCN5A mutations can give origin to different conditions ranging from Long QT Syndrome, to BrS, to progressive cardiac conduction defect, to Dilated Cardiomyopathy[34]; mutations on potassium channel genes can cause Short or Long QT syndromes[35]; and several genes for sarcomeric proteins when mutated can cause either Hypertrophic or Dilated Cardiomyopathy[36]. This “multiplicity” of a clinical phenotype is here proposed for the first time for a desmosomal gene, which can associate with a spectrum that includes the BrS phenotype.

PKP2 and the sodium channel complex

Our previous data demonstrated that PKP2 ablation decreased I_{Na} and elicited reentrant arrhythmias in monolayers of cardiomyocytes[5]. We also showed that PKP2-Hz mice had reduced I_{Na} that facilitated flecainide-induced arrhythmias and sudden death[6]. These results support the role of impaired I_{Na} as a mechanism affecting arrhythmia susceptibility in the “concealed” phase of AC. Additional data showed that the intensity of immunoreactive $Na_v1.5$ was reduced in most heart sections obtained from AC patients[7]. This finding, consistent with those of Gomes et al[32], indicate that a reduction in $Na_v1.5$ abundance may be a component of the phenotype in subjects with AC.

The role of PKP2 in preserving I_{Na} may be independent from its function as a component of the desmosome. Indeed, we speculate that some PKP2 mutations may primarily affect one function while not disrupting –or only minimally disrupting- the other. In fact, although AC is associated with fibrofatty replacement of ventricular muscle, our data suggest that cytoskeletal alterations affecting ion channel trafficking may precede larger scale tissue changes and contribute or even dominate the phenotype. We propose that specific PKP2 mutations can lead to a decreased depolarization reserve that manifests as BrS. Future experiments, using whole animal models, will be necessary to better define the role of PKP2 and other “mechanical junction proteins” in establishing the depolarizing reserve of the mammalian heart.

Previous studies have shown that N-cadherin-containing complexes act as anchoring points for microtubules at the intercalated disc[25]. PKP2 and N-cadherin are both components of the area composita, a “mixed” junction of the adult intercalated disc linked to AC[37]. We show that PKP2 deficiency increases the distance between the microtubule plus-end and the N-cadherin plaque (Figure 8), suggesting that integrity of the area composita as a whole, rather than only N-cadherin, is relevant to microtubule anchoring. The evidence that $Na_V1.5$ is delivered to the cell membrane through the microtubular network[23], and our results showing that reduced I_{Na} is consequent to decreased functional channel expression, lead us to

propose that PKP2 is necessary for microtubule anchoring and safe delivery of $Na_V1.5$ to the ID. Of note, Cx43 is also necessary to preserve I_{Na} amplitude[22], and we recently demonstrated that PKP2 and Cx43 share a subcellular domain[3], forming a molecular network (the connexome). Whether this domain (likely at the perinexus[38]) constitutes an actual point of anchoring and delivery for microtubules, deserves further investigation.

Conclusions

This manuscript represents the first systematic retrospective analysis of a large patient population with diagnosis of BrS to define the co-existence of clinical BrS and genetic variations in *PKP2*. This is also the first study demonstrating that not only the absence of PKP2, but also single amino acid mutations in its sequence, can alter I_{Na}. We propose that *PKP2* mutations provide at least part of the molecular substrate of BrS. Whether co-existence of *PKP2* mutations and a positive flecainide test have value in assessing sudden death risk and/or progression toward cardiomyopathy, is unclear. The inclusion of PKP2 as part of routine BrS genetic testing remains premature; yet, the possibility that some patients showing signs of disease may harbor PKP2 variants should be considered when the genotype is negative for other genes associated with BrS.

Supplementary Material

Refer to Web version on PubMed Central for supplementary material.

Acknowledgments

Funding Sources: This work was supported by grants NIH-HL106632, NIH-GM057691, Leducq Foundation (MD); Telethon-GGP1114/GGP06007, Leducq Foundation-08CVD01, PRIN-2010BWY8E9 (SP/CN); NIH-HL105194, CIRM-RB2-01512, RB4-06276 (H-S.V.C).

References

1. van Tintelen JP, Entius MM, Bhuiyan ZA, Jongbloed R, Wiesfeld AC, Wilde AA, van der Smagt J, Boven LG, Mannens MM, van Langen IM, Hofstra RM, Otterspoor LC, Doevendans PA, Rodriguez LM, van Gelder IC, Hauer RN. Plakophilin-2 mutations are the major determinant of familial arrhythmogenic right ventricular dysplasia/cardiomyopathy. Circulation. 2006; 113:1650–1658. [PubMed: 16567567]
2. Oxford EM, Musa H, Maass K, Coombs W, Taffet SM, Delmar M. Connexin43 remodeling caused by inhibition of plakophilin-2 expression in cardiac cells. Circ res. 2007; 101:703–711. [PubMed: 17673670]
3. Agullo-Pascual E, Reid DA, Keegan S, Sidhu M, Fenyo D, Rothenberg E, Delmar M. Super-resolution fluorescence microscopy of the cardiac connexome reveals plakophilin-2 inside the connexin43 plaque. Cardiovasc res. 2013; 100:231–240. [PubMed: 23929525]
4. Sato PY, Coombs W, Lin X, Nekrasova O, Green KJ, Isom LL, Taffet SM, Delmar M. Interactions between ankyrin-g, plakophilin-2, and connexin43 at the cardiac intercalated disc. Circ res. 2011; 109:193–201. [PubMed: 21617128]
5. Sato PY, Musa H, Coombs W, Guerrero-Serna G, Patino GA, Taffet SM, Isom LL, Delmar M. Loss of plakophilin-2 expression leads to decreased sodium current and slower conduction velocity in cultured cardiac myocytes. Circ res. 2009; 105:523–526. [PubMed: 19661460]
6. Cerrone M, Noorman M, Lin X, Chkourko H, Liang FX, van der Nagel R, Hund T, Birchmeier W, Mohler P, van Veen TA, van Rijen HV, Delmar M. Sodium current deficit and arrhythmogenesis in a murine model of plakophilin-2 haploinsufficiency. Cardiovasc res. 2012; 95:460–468. [PubMed: 22764151]
7. Noorman M, Hakim S, Kessler E, Groeneweg J, Gpj Cox M, Asimaki A, van Rijen HV, van Stuijvenberg L, Chkourko H, van der Heyden MA, Vos MA, de Jonge N, van der Smagt JJ, Dooijes D, Vink A, de Weger RA, Varro A, de Bakker JM, Saffitz JE, Hund TJ, Mohler PJ, Delmar M,

Hauer RN, van Veen TA. Remodeling of the cardiac sodium channel, connexin43 and plakoglobin at the intercalated disk in patients with arrhythmogenic cardiomyopathy. Heart rhythm. 2012; 10:412–419. [PubMed: 23178689]

8. Chen Q, Kirsch GE, Zhang D, Brugada R, Brugada J, Brugada P, Potenza D, Moya A, Borggrefe M, Breithardt G, Ortiz-Lopez R, Wang Z, Antzelevitch C, O'Brien RE, Schulze-Bahr E, Keating MT, Towbin JA, Wang Q. Genetic basis and molecular mechanism for idiopathic ventricular fibrillation. Nature. 1998; 392:293–296. [PubMed: 9521325]
9. Bhargava A, Lin X, Novak P, Mehta K, Korchev Y, Delmar M, Gorelik J. Super-resolution scanning patch clamp reveals clustering of functional ion channels in adult ventricular myocyte. Circ res. 2013; 112:1112–1120. [PubMed: 23438901]
10. Claycomb WC, Lanson NA Jr, Stallworth BS, Egeland DB, Delcarpio JB, Bahinski A, Izzo NJ Jr. Hl-1 cells: A cardiac muscle cell line that contracts and retains phenotypic characteristics of the adult cardiomyocyte. Proc Natl Acad Sci USA. 1998; 95:2979–2984. [PubMed: 9501201]
11. Chkourko HS, Guerrero-Serna G, Lin X, Darwish N, Pohlmann JR, Cook KE, Martens JR, Rothenberg E, Musa H, Delmar M. Remodeling of mechanical junctions and of microtubule-associated proteins accompany cardiac connexin 43 lateralization. Heart Rhythm. 2012; 9:1133–1140. e1136. [PubMed: 22406144]
12. Kim C, Wong J, Wen J, Wang S, Wang C, Spiering S, Kan NG, Forcales S, Puri PL, Leone TC, Marine JE, Calkins H, Kelly DP, Judge DP, Chen HS. Studying arrhythmogenic right ventricular dysplasia with patient-specific ipscs. Nature. 2013; 494:105–110. [PubMed: 23354045]
13. Awad MM, Dalal D, Tichnell C, James C, Tucker A, Abraham T, Spevak PJ, Calkins H, Judge DP. Recessive arrhythmogenic right ventricular dysplasia due to novel cryptic splice mutation in pkp2. Hum mut. 2006; 27:1157. [PubMed: 17041889]
14. Norton N, Robertson PD, Rieder MJ, Zuchner S, Rampersaud E, Martin E, Li D, Nickerson DA, Hershberger RE. Evaluating pathogenicity of rare variants from dilated cardiomyopathy in the exome era. Circ Cardiovasc genet. 2012; 5:167–174. [PubMed: 22337857]
15. van der Zwaag PA, Jongbloed JD, van den Berg MP, van der Smagt JJ, Jongbloed R, Bikker H, Hofstra RM, van Tintelen JP. A genetic variants database for arrhythmogenic right ventricular dysplasia/cardiomyopathy. Hum mut. 2009; 30:1278–1283. [PubMed: 19569224]
16. Christensen AH, Benn M, Bundgaard H, Tybjaerg-Hansen A, Haunso S, Svendsen JH. Wide spectrum of desmosomal mutations in danish patients with arrhythmogenic right ventricular cardiomyopathy. J med genet. 2010; 47:736–744. [PubMed: 20864495]
17. Bauce B, Nava A, Beffagna G, Basso C, Lorenzon A, Smaniotto G, De Bortoli M, Rigato I, Mazzotti E, Steriotis A, Marra MP, Towbin JA, Thiene G, Danieli GA, Rampazzo A. Multiple mutations in desmosomal proteins encoding genes in arrhythmogenic right ventricular cardiomyopathy/dysplasia. Heart rhythm. 2010; 7:22–29. [PubMed: 20129281]
18. Lahtinen AM, Lehtonen E, Marjamaa A, Kaartinen M, Helio T, Porthan K, Oikarinen L, Toivonen L, Swan H, Jula A, Peltonen L, Palotie A, Salomaa V, Kontula K. Population-prevalent desmosomal mutations predisposing to arrhythmogenic right ventricular cardiomyopathy. Heart rhythm. 2011; 8:1214–1221. [PubMed: 21397041]
19. Antzelevitch C, Brugada P, Borggrefe M, Brugada J, Brugada R, Corrado D, Gussak I, LeMarec H, Nademanee K, Perez Riera AR, Shimizu W, Schulze-Bahr E, Tan H, Wilde A. Brugada syndrome: Report of the second consensus conference: Endorsed by the Heart Rhythm Society and the European Heart Rhythm Association. Circulation. 2005; 111:659–670. [PubMed: 15655131]
20. Mao W, You T, Ye B, Li X, Dong HH, Hill JA, Li F, Xu H. Reactive oxygen species suppress cardiac nav1.5 expression through foxo1. PloS one. 2012; 7:e32738. [PubMed: 22400069]
21. Lin X, Liu N, Lu J, Zhang J, Anumonwo JM, Isom LL, Fishman GI, Delmar M. Subcellular heterogeneity of sodium current properties in adult cardiac ventricular myocytes. Heart Rhythm. 2011; 8:1923–1930. [PubMed: 21767519]
22. Lubkemeier I, Requardt RP, Lin X, Sasse P, Andrie R, Schrickel JW, Chkourko H, Bukauskas FF, Kim JS, Frank M, Malan D, Zhang J, Wirth A, Dobrowolski R, Mohler PJ, Offermanns S, Fleischmann BK, Delmar M, Willecke K. Deletion of the last five c-terminal amino acid residues of connexin43 leads to lethal ventricular arrhythmias in mice without affecting coupling via gap junction channels. Basic res card. 2013; 108:348.

23. Casini S, Tan HL, Demirayak I, Remme CA, Amin AS, Scicluna BP, Chatyan H, Ruijter JM, Bezzina CR, van Ginneken AC, Veldkamp MW. Tubulin polymerization modifies cardiac sodium channel expression and gating. Cardiovasc res. 2010; 85:691–700. [PubMed: 19861310]
24. O'Brien JE, Sharkey LM, Vallianatos CN, Han C, Blossom JC, Yu T, Waxman SG, Dib-Hajj SD, Meisler MH. Interaction of voltage-gated sodium channel nav1.6 (scn8a) with microtubule-associated protein map1b. J biol chem. 2012; 287:18459–18466. [PubMed: 22474336]
25. Shaw RM, Fay AJ, Puthenveedu MA, von Zastrow M, Jan YN, Jan LY. Microtubule plus-end-tracking proteins target gap junctions directly from the cell interior to adherens junctions. Cell. 2007; 128:547–560. [PubMed: 17289573]
26. Rizzo S, Lodder EM, Verkerk AO, Wolswinkel R, Beekman L, Pilichou K, Basso C, Remme CA, Thiene G, Bezzina CR. Intercalated disc abnormalities, reduced Na(+) current density, and conduction slowing in desmoglein-2 mutant mice prior to cardiomyopathic changes. Cardiovasc Res. 2012; 95:409–418. [PubMed: 22764152]
27. Ackerman MJ, Priori SG, Willems S, Berul C, Brugada R, Calkins H, Camm AJ, Ellinor PT, Gollob M, Hamilton R, Hershberger RE, Judge DP, Le Marec H, McKenna WJ, Schulze-Bahr E, Semsarian C, Towbin JA, Watkins H, Wilde A, Wolpert C, Zipes DP. HRS/EHRA expert consensus statement on the state of genetic testing for the channelopathies and cardiomyopathies this document was developed as a partnership between the Heart Rhythm Society (HRS) and the European Heart Rhythm Association (EHRA). Heart rhythm. 2011; 8:1308–1339. [PubMed: 21787999]
28. Corrado D, Basso C, Buja G, Nava A, Rossi L, Thiene G. Right bundle branch block, right precordial ST-segment elevation, and sudden death in young people. Circulation. 2001; 103:710–717. [PubMed: 11156883]
29. Catalano O, Antonaci S, Moro G, Mussida M, Frascaroli M, Baldi M, Cobelli F, Baiardi P, Nastoli J, Bloise R, Monteforte N, Napolitano C, Priori SG. Magnetic resonance investigations in Brugada syndrome reveal unexpectedly high rate of structural abnormalities. Eur heart j. 2009; 30:2241–2248. [PubMed: 19561025]
30. Gerull B, Heuser A, Wichter T, Paul M, Basson CT, McDermott DA, Lerman BB, Markowitz SM, Ellinor PT, MacRae CA, Peters S, Grossmann KS, Drenckhahn J, Michely B, Sasse-Klaassen S, Birchmeier W, Dietz R, Breithardt G, Schulze-Bahr E, Thierfelder L. Mutations in the desmosomal protein plakophilin-2 are common in arrhythmogenic right ventricular cardiomyopathy. Nature genet. 2004; 36:1162–1164. [PubMed: 15489853]
31. Zhang M, Tavora F, Oliveira JB, Li L, Franco M, Fowler D, Zhao Z, Burke A. Pkp2 mutations in sudden death from arrhythmogenic right ventricular cardiomyopathy (ARVC) and sudden unexpected death with negative autopsy (SUDNA). Circulation j. 2012; 76:189–194.
32. Gomes J, Finlay M, Ahmed AK, Ciaccio EJ, Asimaki A, Saffitz JE, Quarta G, Nobles M, Syrris P, Chaubey S, McKenna WJ, Tinker A, Lambiase PD. Electrophysiological abnormalities precede overt structural changes in arrhythmogenic right ventricular cardiomyopathy due to mutations in desmoplakin-a combined murine and human study. European Heart J. 2012; 33:1942–1953. [PubMed: 22240500]
33. Kaplan SR, Gard JJ, Protonotarios N, Tsatsopoulou A, Spiliopoulou C, Anastasakis A, Squarcioni CP, McKenna WJ, Thiene G, Basso C, Brousse N, Fontaine G, Saffitz JE. Remodeling of myocyte gap junctions in arrhythmogenic right ventricular cardiomyopathy due to a deletion in plakoglobin (Naxos disease). Heart rhythm. 2004; 1:3–11. [PubMed: 15851108]
34. Ruan Y, Liu N, Priori SG. Sodium channel mutations and arrhythmias. Nature reviews. Cardiology. 2009; 6:337–348.
35. Cerrone M, Napolitano C, Priori SG. Genetics of ion-channel disorders. Current op cardiol. 2012; 27:242–252.
36. Morimoto S. Sarcomeric proteins and inherited cardiomyopathies. Cardiovasc Res. 2008; 77:659–666. [PubMed: 18056765]
37. van Hengel J, Calore M, Bauce B, Dazzo E, Mazzotti E, De Bortoli M, Lorenzon A, Li Mura IE, Beffagna G, Rigato I, Vleeschouwers M, Tyberghein K, Hulpiau P, van Hamme E, Zaglia T, Corrado D, Basso C, Thiene G, Daliento L, Nava A, van Roy F, Rampazzo A. Mutations in the area composita protein alphat-catenin are associated with arrhythmogenic right ventricular cardiomyopathy. Eur Heart J. 2013; 34:201–210. [PubMed: 23136403]

38. Rhett JM, Gourdie RG. The perinexus: A new feature of cx43 gap junction organization. Heart rhythm. 2012; 9:619–623. [PubMed: 21978964]

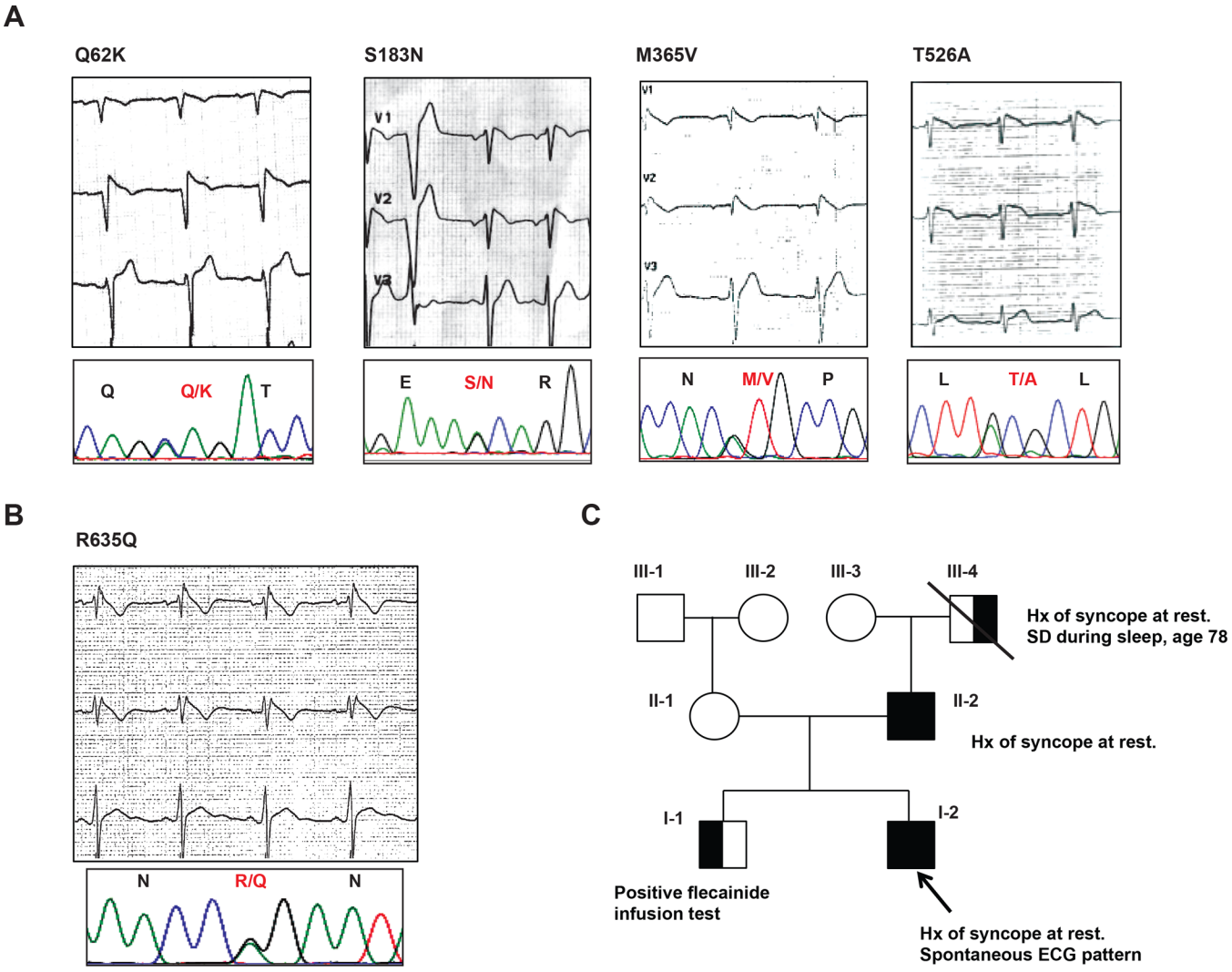

Figure 1.

A: top: ECG showing coved-type ST elevation in leads V1–V2 in patients carriers of PKP2 variants. Q62K, M365V and T526A carriers showed flecainide-induced ECG; S183N carrier showed spontaneous ECG pattern during febrile episode. Bottom: correspondent DNA sequence showing heterozygous missense variants in *PKP2*. B: left: Spontaneous coved-type ECG in carrier of variant R635Q, and corresponding DNA sequence. Right: pedigree showing co-segregation between genotype and clinical phenotype in this family. Symbols: square, male; circle, female; solid, gene-carrier with clinical symptoms; empty, asymptomatic, negative genotype; half-full left, gene-carrier; half-full right, clinical symptoms.

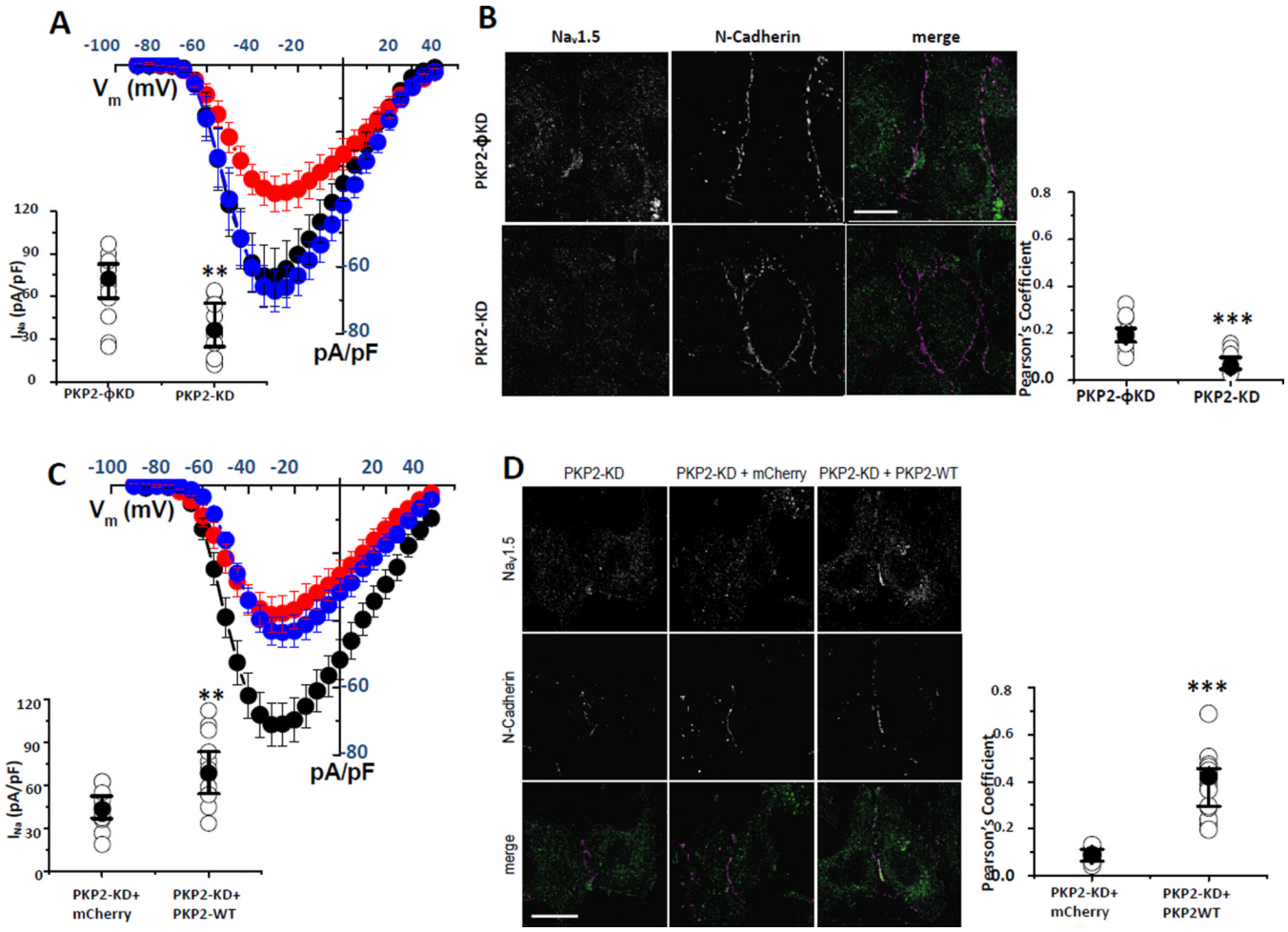

Figure 2.

A: Average peak I_{Na} density as a function of voltage command in HL-1 cells WT (black symbols; n=11), treated with PKP2 silencing construct (PKP2-KD; red; n=12), and treated with a non-silencing construct (PKP2-ϕKD; blue; n=12). For display purposes only, these data are shown as mean +/− standard error of the mean (SEM). Statistical comparisons were carried out by MWW test and limited to peak I_{Na} density at −30 mV for PKP2-KD vs. PKP2-ϕKD. The corresponding dot plot is shown in the inset. **p<0.005. B: $Na_V1.5$ (green in merge) and N-Cadherin (pink in merge) decreased in PKP2-KD and not in PKP2-ϕKD cells. Right panel: Pearson's coefficient dot plots, ***p<0.0005 (n=12 for each group). C: Average peak I_{Na} density in PKP2-KD cells (red line and symbols; n=12) increased when cells were transfected with PKP2-WT (black; PKP2-KD+PKP2-WT; n=13) but not when PKP2-KD cells were transfected with mCherry (blue; n=11). Inset shows data plot (same format as in A) for comparison of PKP2-KD+mCherry vs PKP2-KD+PKP2-WT; **p<0.005. D: co-localization of $Na_V1.5$ (green) with N-Cadherin (pink) rescued by transfection of PKP2-KD cells with wild-type construct (PKP2-KD+PKP2-WT), but not by transfection of mCherry alone (PKP2-KD+mCherry). Pearson's coefficient dot plot on the right. ***p<0.0001 when comparing PKP2-KD+mCherry (n=12) against PKP2-KD+PKP2-WT (n=16). Scale bars in B and D: 20 μm.

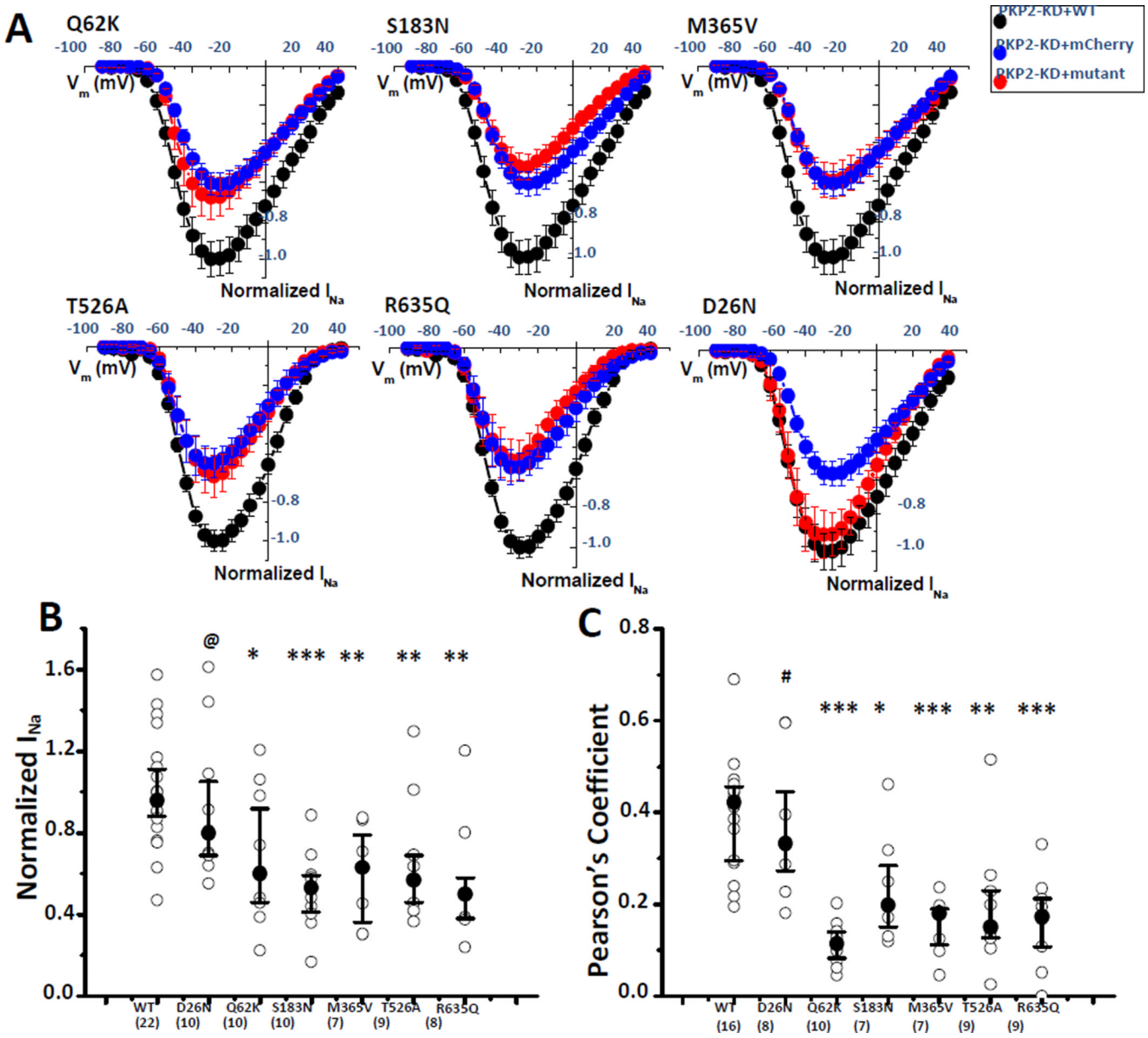

Figure 3.

A: Peak I_{Na} as function of voltage in PKP2-KD cells (blue), PKP2-KD cells transfected with wild-type PKP2 (black; PKP2-KD+PKP2-WT) and cells transfected with different PKP2 variants (red). Additional I_{Na} properties, supplemental figures 4,5. Data are presented as mean+/− SEM for display purposes only. B: Dot plots of peak I_{Na} density at −30 mV measured for each mutant. C: Pearson coefficient values showing loss of $Na_V1.5$ and N-cadherin co-localization for cells transfected with 5 PKP2 mutants, and maintained co-localization in cells transfected with WT or D26N. For B and C: *p<0.05; **p<0.01; *** p<0.001; $^{@}$p=0.28; $^{\#}$p=0.48. Each variant was compared separately against the WT group. n values in parentheses under each column.

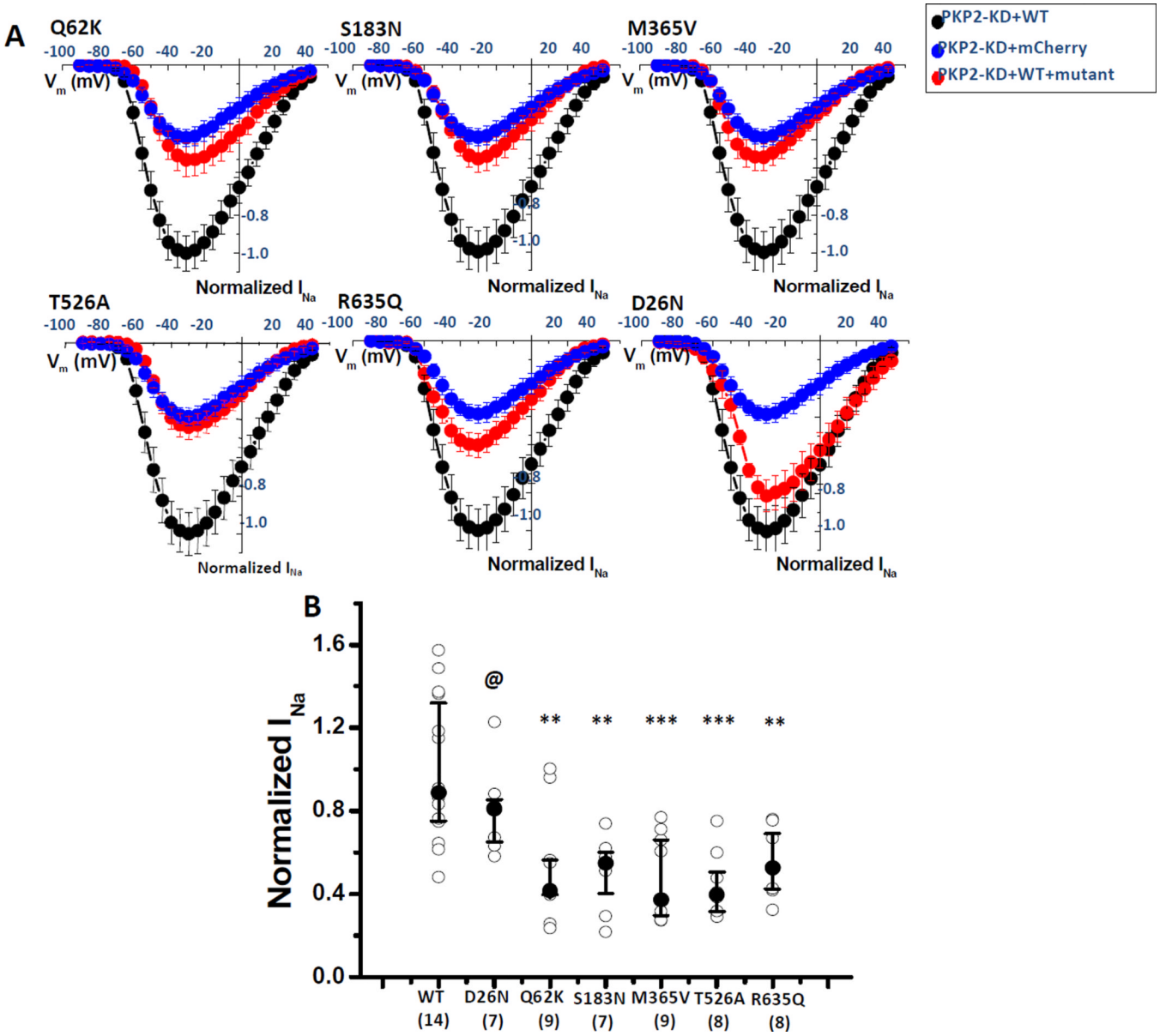

Figure 4.

A: Peak I_{Na} as function of voltage in PKP2-KD cells (blue; cells transfected with mCherry), PKP2-KD cells transfected with wild-type PKP2 (black) and cells transfected with PKP2WT and a PKP2 variant (red). For co-expression, 1:1 plasmid ratio was used. For WT controls, WT plasmid was equal to the sum of WT+variant in test set. Data are presented as mean+/− SEM for display purposes only. B: For statistical analysis (MWW test), each variant was compared separately against group PKP2-KD+WT (n=14). p values were as follows (n values in parentheses): PKP2-KD+WT+Q62K (n=9): $p<0.01$; PKP2-KD+WT+S183N (n=7): $p<0.005$; PKP2-KD+WT+M365V (n=9): $p<0.001$; PKP2-KD+WT+T526A (n=8): $p<0.001$; PKP2-KD+WT+R635Q (n=8): $p<0.005$. PKP2-KD+WT+D26N (n=7): $p=0.12$ (NS).

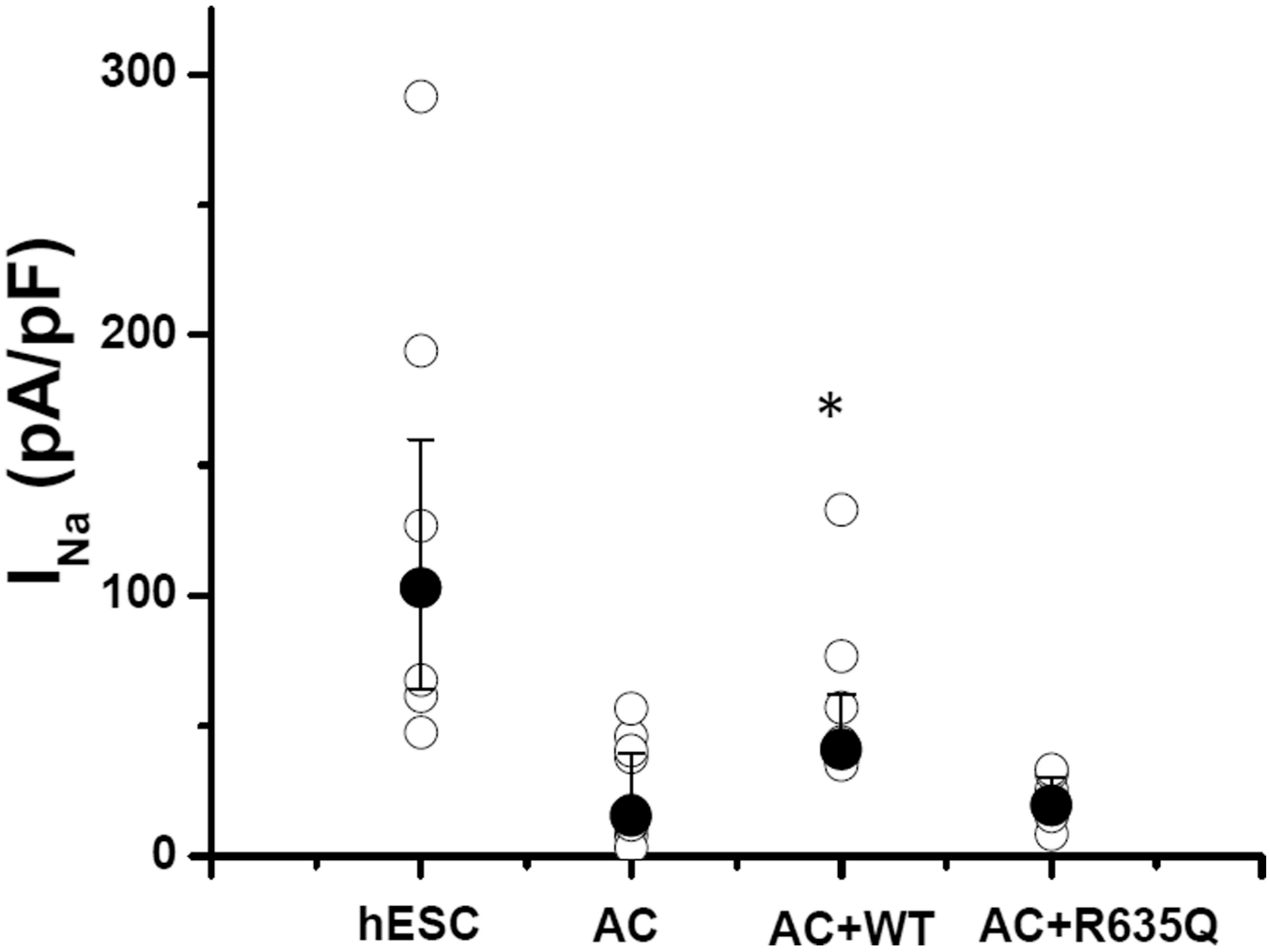

Figure 5.

Dot plot of I_{Na} density for voltage clamp pulse to −20 mV from a holding potential of −120 mV in WT-hESC-CMs (hESC;n=7), AC-hIPSC-CMs (AC;n=8), AC-hIPSC-CMs+PKP2-WT (AC+WT;n=8), and hIPSC-CMs+PKP2-R635Q (AC+R635Q;n=10). AC vs AC-WT, *p<0.05; AC vs AC-R635Q, p=0.85 (NS). Recordings limited to one voltage amplitude, as acceptable recordings (tight and stable gigohm seals and reproducible current traces) were short-lived.

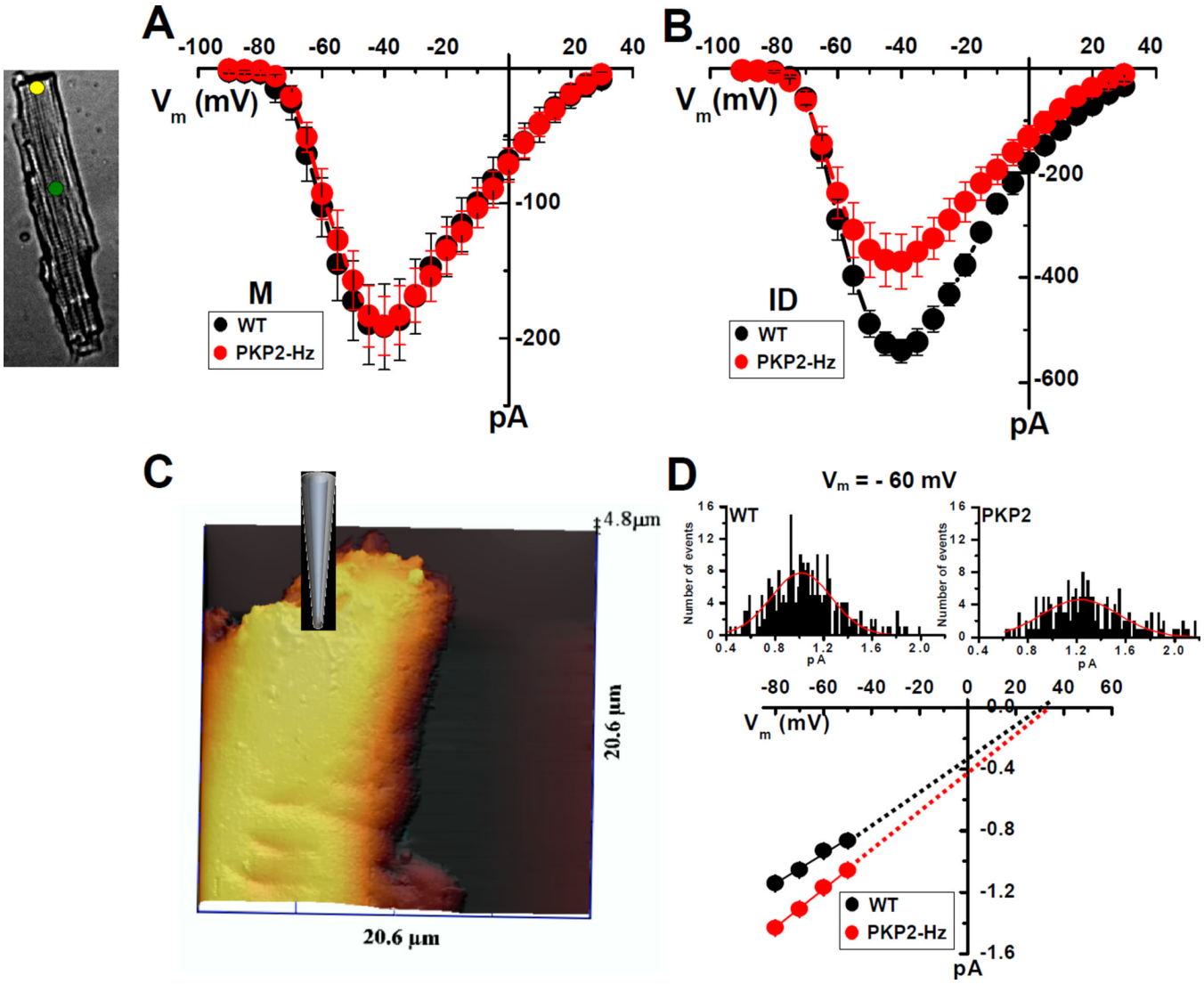

Figure 6.

A,B: Peak average I_{Na} in macropatches from cell midsection (A; green circle in left inset; n=10 for each group) or from the region previously occupied by the ID (B; yellow circle in left inset; n=7 for WT and 9 for PKP2-Hz). Data are presented as mean+/− SEM for display purposes only. Dot plots comparing I_{Na} density at −30 mV in online Figure 12; $p<0.05$ for ID recordings, and $p=0.97$ (NS) for M. C: SICM recording of the end of an adult ventricular myocyte. Notice (from bottom to top) the last striations and then a smooth, T-tubule-free region, closer to cell end. D: Single sodium channel data from either WT, or PKP2-Hz cells. Methodological details in[9].

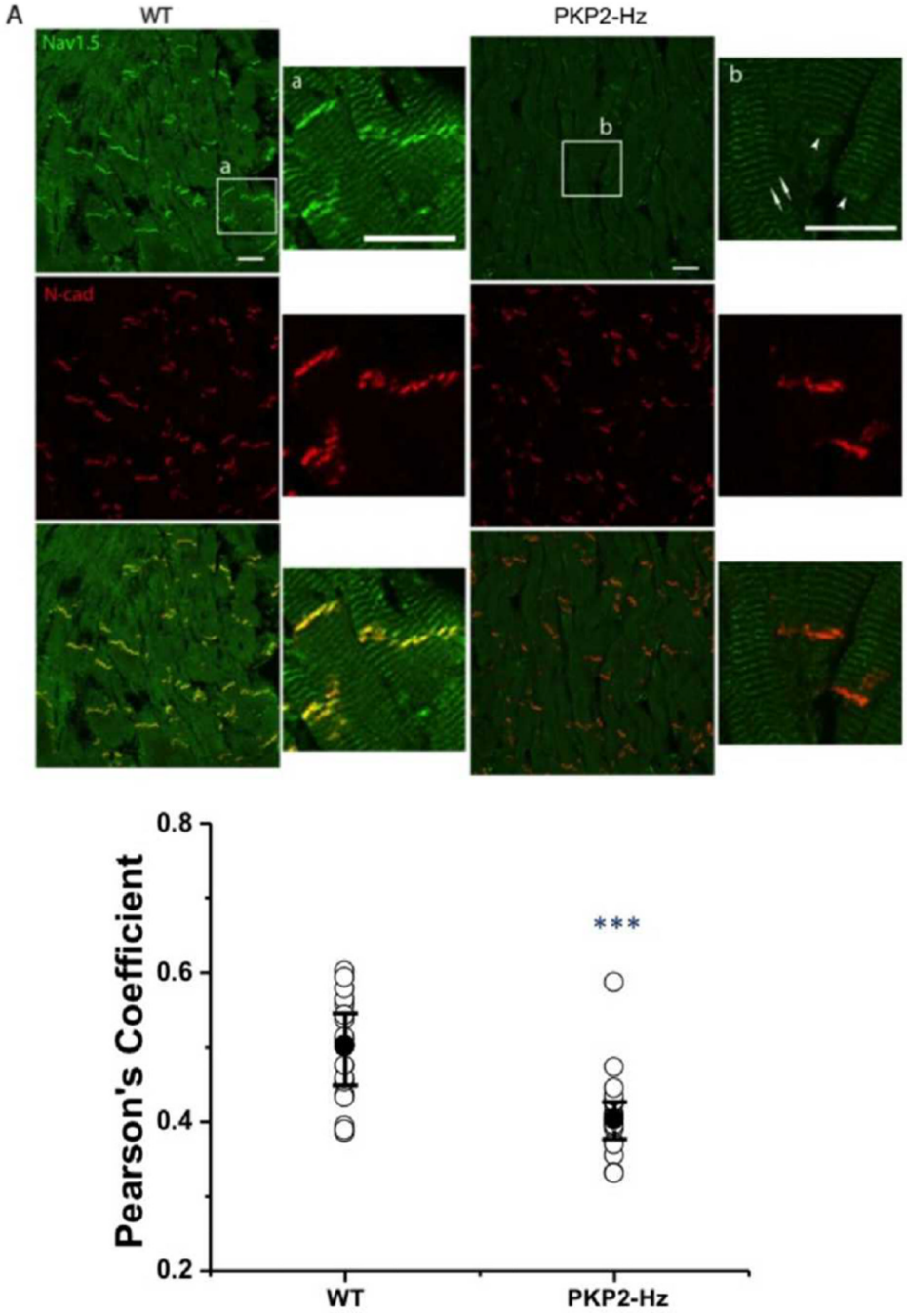

Figure 7.

A: Co-localization of N-Cadherin (red) and $Na_V1.5$ (green) by conventional fluorescence microscopy in adult ventricular tissue from PKP2-Hz mice (right; PKP2+/−) and control littermate (left; WT). Inset in "a" shows brighter signal indicating localization at the ID; long arrows in "b" show staining along striations; arrowheads show decreased staining intensity at ID. B: Dot plot of Pearson's coefficient showing decreased N-cadherin/$Na_V1.5$ co-localization in PKP2-Hz. n values were 20 for WT and 18 for PKP2-Hz ($p<0.001$). Same methods as in.[22] For further details see online supplement.

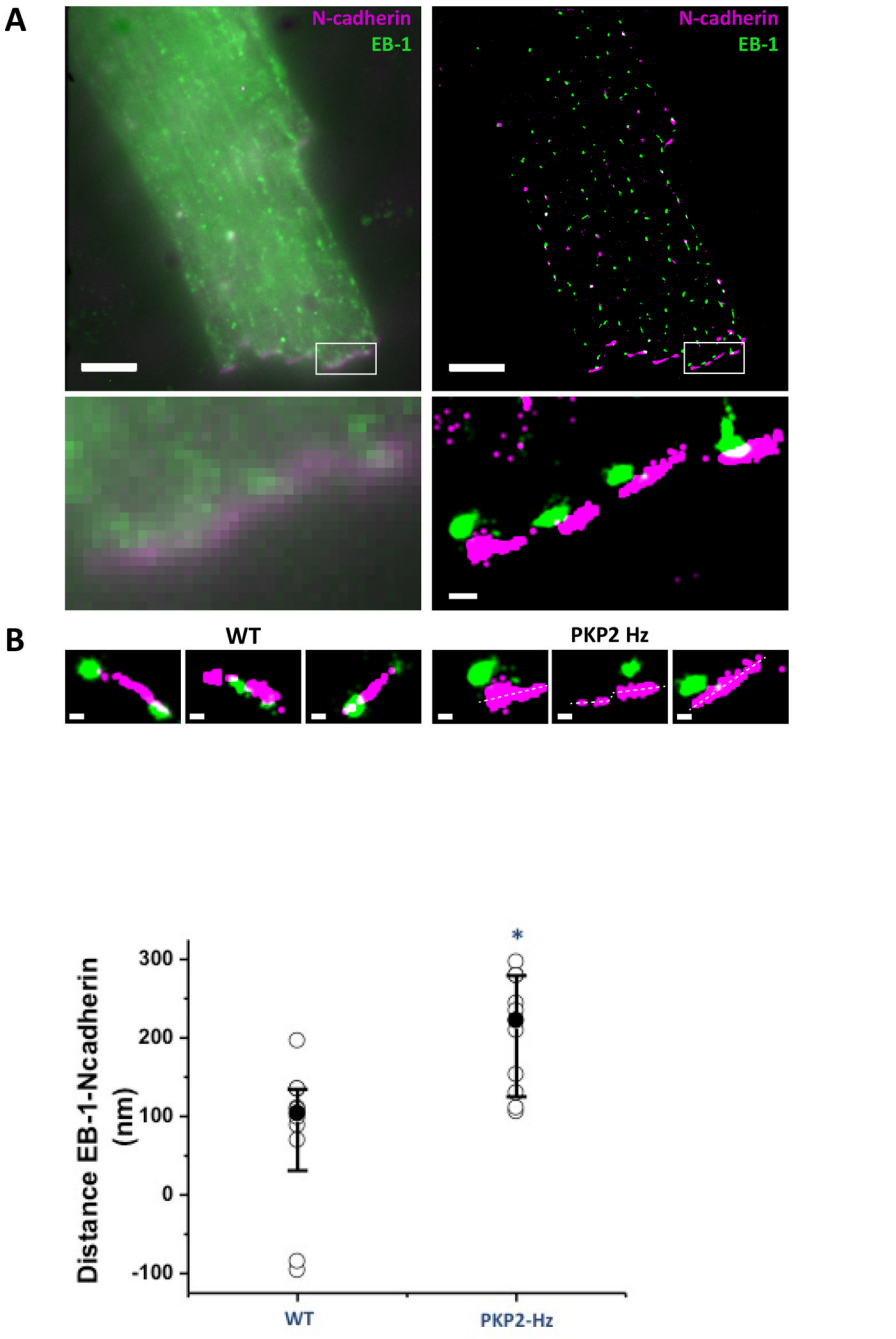

Figure 8.

Localization of EB-1 (green) and N-cadherin (purple) in adult ventricular myocytes. A: Image by TIRF (left) or dSTORM (right). Inset enlarged in bottom panels to show increased resolution. B: clusters in WT (left) are closer to each other than in PKP2-Hz cells (right). C: Dot plot of distance from EB-1 to N-cadherin showing increased separation between the proteins in the PKP2-Hz cells. n values for statistical comparison were 10 for WT and 10 for PKP2-Hz. *$p<0.005$. For further details see[3] and online supplement.